Intrinsic thermal conductivity in monolayer graphene is ultimately upper limited: A direct estimation by atomistic simulations

Giuliana Barbarino,* Claudio Melis,† and Luciano Colombo‡
Dipartimento di Fisica, Università di Cagliari, Cittadella Universitaria, I-09042 Monserrato (Ca), Italy
(Received 5 November 2014; published 13 January 2015)

In the sample size domain so far explored, the thermal conductivity of graphene shows an intriguing dependence on the sample length L_z along the heat flux direction. An extrapolated infinite value for such a thermal conductivity is sometimes suggested for infinite samples, while other investigations predict anyway an upper limit for it. We address this issue by avoiding any guess or approximation on the underlying microscopic heat transport mechanisms; we rather perform direct atomistic simulations aimed at estimating thermal conductivity in samples with increasing size up to the unprecedented value of $L_z = 0.1$ mm. Our results provide evidence that thermal conductivity in graphene is definitely upper limited in samples long enough to allow a diffusive transport regime for both single and collective phonon excitations.

DOI: 10.1103/PhysRevB.91.035416 PACS number(s): 65.80.Ck, 63.22.Rc, 31.15.xv

Since the first measure of the thermal conductivity κ in graphene, reporting an extremely high value [1], several experimental and theoretical investigations have been focused on the characterization of the thermal properties of this atomic monolayer. However, it is still difficult to assign a sharp value to κ since the experimental measurements scatter between 600 and 5000 $\mathrm{W\,m^{-1}\,K^{-1}}$ depending on different samples quality [1–5]. In order to rationalize this experimental scenario, several theoretical models [6–8] have been numerically implemented by means of *ab initio* [9–12] or model-potential [13,14] calculations. Direct equilibrium and nonequilibrium molecular dynamics (MD) simulations [15–17] have been as well addressed to estimate κ. Overall, κ has been theoretically predicted to vary in the range 300–3596 $\mathrm{W\,m^{-1}\,K^{-1}}$.

Most investigations underline the dominant role in the transport of heat played by acoustic phonons, showing in graphene three polarizations: the longitudinal (LA) and the transverse (TA) ones, both associated to in-plane vibrations, and the flexural one (ZA) due to out-of-plane oscillations. Although it has been guessed that only in-plane phonons carry heat [18,19], more recently it has been recognized that the ZA phonons are in fact fundamental in graphene thermal transport [3,10,11,14,17]: despite that they show a very low group velocity and Gruinesen parameter, their lifetime is comparatively very long due to a selection rule for three-phonon scattering.

Another exotic feature of graphene thermal transport, which has been predicted by several theoretical works [12,14,16,18] and recently observed by experiments [20], is the $\kappa = \kappa(L_z)$ dependence on the sample length L_z along the heat flux direction, for which different interpretations have been supplied. In MD simulations the $\kappa(L_z)$ dependence is commonly attributed [17,21] to a well-known size effect hindering those phonons having a mean free path (MFP) longer than L_z (corresponding to the dimension of the periodically repeated simulation cell). Eventually this results in an artificial ballistic transport regime. This is typically the case of equilibrium (EMD) [17] or approach-to-equilibrium (AEMD) [22] simulations, as schematically shown in Fig. 1. As for nonequilibrium MD (NEMD), this dependence is in turn generated by the presence of two thermostats at the sample boundaries of the finite-size simulated sample [16]. In any case, a reliable description of the intrinsic thermal conductivity needs the achievement of a truly diffusive regime, a situation that can only be reached by increasing the size of the simulation cell up to a system-dependent critical length L_{diff}. This is the length at which phonon dynamics becomes diffusive for all modes; until recently, L_{diff} in graphene was reported to range 1–10 μm [10].

A different situation is found in lattice dynamics calculations in the long-wavelength approximation (LWA), such as in Klemens-like models [8,18,23]: here the $\kappa(L_z)$ dependence is artificially included by construction, through the definition of a cutoff frequency $\omega_{\mathrm{min}} \propto \sqrt{1/L_z}$ which was first introduced by Klemens to adapt the thermal transport description given for graphite to graphene where the transport is intrinsically two dimensional (2D) even for small phonon frequencies. In this case the low-bound cutoff frequency is determined by the condition that the phonon MFP cannot exceed the physical size L_z of a graphene sample.

Finally, an explicit $\kappa(L_z)$ dependence for $L_z \leqslant 50$ μm is also found by exactly solving the Boltzmann transport equation (BTE) [14]. Here an empirical length-dependent rate is introduced to count boundary scatterings in a finite-size sample [9].

An experimental evidence of the $\kappa(L_z)$ dependence has been recently shown by thermal resistance measurements on single-layer graphene samples [20] suspended between two SiN membranes (one used as an heater, the other as sensor) to measure the temperature rise at the end of the sample (see Fig. 1): a $\kappa \sim \log L_z$ dependence was observed for sample lengths up to 9 μm.

Even if both experiments and theory agree in predicting a L_z-dependent thermal conductivity in the sample size domain so far investigated, an active debate about its possible divergence for $L_z \to \infty$ is presently ongoing in the literature. In particular, theoretical models only taking into account in-plane phonon modes (disregarding, therefore, out-of-plane flexural modes) predict a logarithmic divergence at room

*giuliana.barbarino@dsf.unica.it
†claudio.melis@dsf.unica.it
‡luciano.colombo@dsf.unica.it

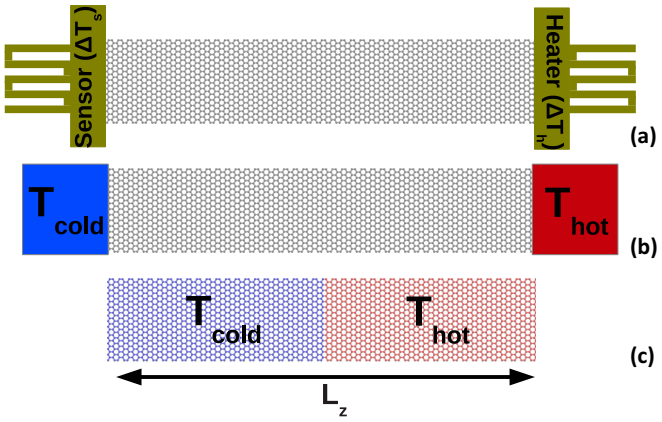

FIG. 1. (Color online) Schematic representation of the characteristic length L_z in different situations: (a) typical setup of an experimental thermal resistance measurement; (b) typical geometry for a NEMD simulation; (c) typical geometry of an AEMD simulation (we show the initial configuration where the left and right regions are thermostatted, respectively, at cold and hot temperature).

temperature [8]. Recently this has been confirmed in Ref. [20] by experiments performed on samples with $L_z \leqslant 9$ μm and interpreted as due to the 2D nature of phonons in graphene, as well as to their actual statistical distribution. In particular, it has been argued that the differences in phonon populations between nonequilibrium and equilibrium conditions promote the observed logarithmic divergence.

This conclusion (based on general arguments [24] valid for 2D systems) has been questioned in the specific case of graphene. In fact, it has been argued [12] that, even by assuming $\kappa = \kappa(L_z)$ as due to a regime of ballistic phonon transport in samples with $L_z < L_{\rm diff}$, an upper limit for thermal conductivity should be anyhow reached for long enough samples where a fully diffusive regime can be eventually reached. It has also been calculated that such a diffusive regime is reached only for mm-long samples that can accommodate both single-phonon and collective excitations with typical MFP of $\sim$1 μm [10,11] and $\sim$100 μm [12], respectively. The actual occurrence of a truly diffusive regime in mm-long systems has not yet been confirmed since both experiments and MD simulations (of any kind) explored so far much smaller samples.

In this work we offer some insight on this problem by performing unbiased (i.e., with no *a priori* guess) AEMD simulations [25,26] on pristine graphene monolayers with L_z up to a size of 0.1 mm. Our goal is to ultimately state whether the claimed $\kappa \sim \log L_z$ divergence is indeed observed by a direct numerical estimate and, if so, whether this behavior drives to a divergent thermal conductivity for arbitrarily long samples. The present discussion could provide a motivation to perform experimental measurements on mm-long samples.

All the simulations here discussed were performed by imposing an initial nonequilibrium condition to a monolayer graphene sample which was then let free to evolve towards equilibrium by a microcanonical simulation [25]. In particular, we initially set a steplike temperature profile along the z direction by thermostatting the left and right regions of the simulation cells at, respectively, a cold T_2 and hot T_1 temperature (Fig. 1). During the following microcanonical run, the time-dependent difference $\Delta T_C(t)$ between the average temperatures of the two regions was calculated straightforwardly. On the other hand, by solving the heat equation under the above initial boundary conditions, the same difference has been calculated analytically as $\Delta T_A(t) = \sum_{n=1}^{\infty} C_n e^{-\alpha_n^2 \bar{\kappa} t}$, where $\bar{\kappa} = \kappa/\rho c_v$ is the thermal diffusivity of the system with density ρ and specific heat c_v and both $\alpha_n = 2\pi n/L_z$ and the coefficients $C_n = 8(T_1 - T_2)[\cos(\alpha_n L_z/2) - 1]^2/\alpha_n^2 L_z^2$ are determined by the imposed initial conditions. The thermal conductivity κ is easily obtained by setting $\Delta T_C(t) = \Delta T_A(t)$ and using $\bar{\kappa}$ as a fitting parameter. Quantum corrections are duly considered for the specific heat as discussed in Ref. [22]. The present AEMD simulations were performed by using the LAMMPS package [27] with the reactive empirical bond order (REBO) potential in its second generation form [28], whose reliability for graphite has been established [22]. In particular, we remark that the REBO potential ensures a good description of the acoustic branches especially near the Γ point. In the AEMD simulations the equations of motion are integrated by the velocity Verlet algorithm with 1.0-fs time step.

We calculated the thermal conductivity of 13 samples with 0.83 μm $\leqslant L_z \leqslant 100$ μm. The periodic boundary conditions enabled us to simulate an infinite sample in the lateral direction. The corresponding simulation cell spanned the range 24 000–2 880 000 atoms, requiring different simulation times for the AEMD analysis extending from 0.411 to 10 ns.

In Fig. 2 we compare our results with previous NEMD simulations using REBO (circles) and Tersoff (diamonds) empirical potentials, as well as with experimental measurements (triangles) [16,20]. All data sets are in agreement in predicting a logarithmic $\kappa(L_z)$ behavior in the length range

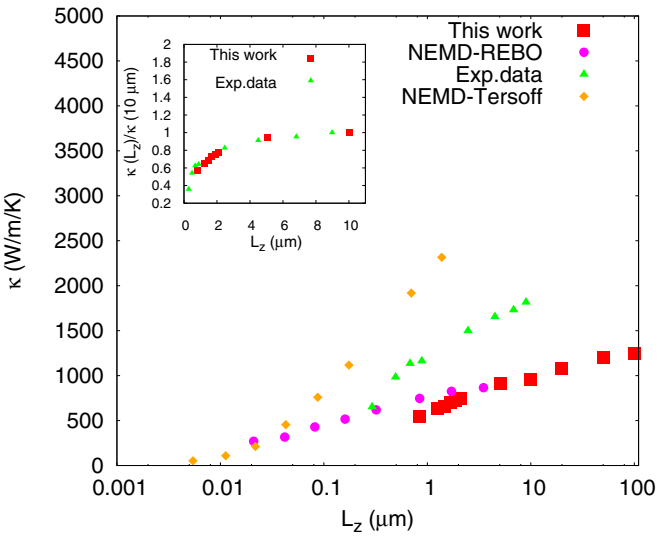

FIG. 2. (Color online) Thermal conductivity $\kappa(L_z)$ of monolayer graphene for increasing sample dimension L_z. Red squares: present AEMD results using REBO potential. Magenta circles: NEMD results using REBO potential (from Ref. [16]). Green triangles: experimental data (from Ref. [20]). Yellow diamonds: NEMD results using Tersoff potential (from Ref. [20]). Inset: AEMD-REBO (red squares) and experimental (green triangles) data normalized to their corresponding value in a reference sample with $L_z = 10$ μm.

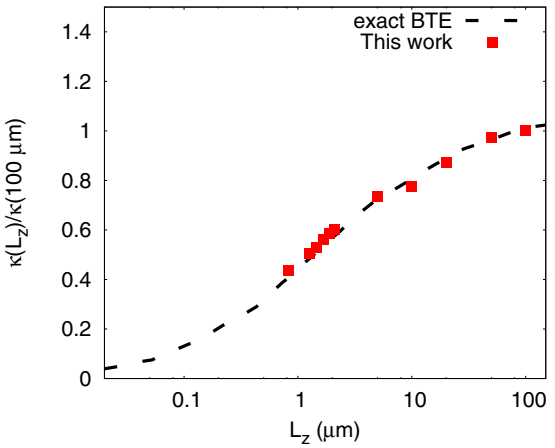

FIG. 3. (Color online) Thermal conductivity $\kappa(L_z)$ of monolayer graphene for increasing sample dimension L_z. Red squares: present AEMD results. Black dashed line: exact solution of BTE provided in Ref. [12]. For sake of comparison, all thermal conductivity values are normalized to $\kappa(100\ \mu\text{m})$, corresponding to a sample with size $L_z = 100\ \mu\text{m}$.

up to 10 μm. However, we remark that the REBO potential provides comparatively smaller absolute values, both in the case of AEMD and NEMD simulations. In order to assess whether this only depends on the accuracy of the empirical potential or it is due to other reasons more fundamentally linked to some heat transport feature, we normalized the REBO values to their corresponding value calculated for a reference sample with $L_z = 10\ \mu$m and compared to (similarly normalized) experimental data. The result is shown in the inset of Fig. 2, proving a really remarkable agreement.

We point out that the AEMD approach can be directly compared to experimental procedures addressing a transient regime, while NEMD simulations are more related a steady-state condition. A more complete analysis should require a direct comparison between results obtained by MD techniques addressing a transient state (such as AEMD) and those addressing a steady state (such as NEMD) in the $1\ \mu\text{m} \leqslant L_z \leqslant 10\ \mu$m range. We guess that these two simulated conditions correspond to different phonon populations, as similarly argued in Ref. [20] by comparing EMD and NEMD predictions of thermal conductivity. This topic, however, falls beyond the scope of the present work and we leave it to a future investigation.

Since the only estimations of κ for sample dimensions greater than $\sim$50 μm are based on the exact *ab initio* solution of the BTE [12], we directly compare AEMD and BTE results in Fig. 3 where, for the same reasons described above, data sets are normalized to their corresponding value for a reference sample with $L_z = 100\ \mu$m. Figure 3 further confirms the reliability of our approach in the description of the κ-vs-L_z trend. More importantly, it provides clear evidence that $\kappa(L_z)$ has indeed an ultimate upper limit, a fact that is now predicted by two independent calculations of rather different nature. This result also confirms the assumption of Ref. [12] which identifies the importance of collective modes (with a comparatively larger MFP than single-phonon ones) to properly define the critical sample length governing the ballistic-to-diffusive transport transition.

Figure 3 clearly shows a change in the $\kappa(L_z)$ trend at about $L_z = 0.1$ mm, indicating that in samples that large heat transport approaches a diffusive regime. This result is consistent with a recent Monte Carlo simulation where μm-long systems are investigated [29]: a ballistic-to-diffusive crossover is captured for a sample length of 0.1 mm. There it is also shown that about 20% of phonons have MFP longer than this length. The picture emerging by combining present AEMD and Monte Carlo simulations is in good agreement with Ref. [12], which indicates $L_{\text{diff}} = 1$ mm as the critical sample length above which is observed a truly diffusive phonon transport regime. We remark that, at variance with previous investigations, in our calculations no educated guesses are used to extract the complex $\kappa(L_z)$ trend. Therefore, we conclude that no $\kappa \sim \log L_z$ divergence in fact occurs in graphene, provided that samples large enough to host a fully diffusive regime are considered. We underline that in order to draw this conclusion out-of-plane oscillations must be duly taken into account, as typical of any MD simulation, since they have a fundamental role in thermal transport. This statement is fully consistent with EMD simulations [20] where such out-of-plane modes were artificially hindered showing that, under such an artificial condition, a divergence of κ vs L_z is indeed found.

In conclusion, we remark that the results of the present AEMD simulations represent direct evidence that κ in graphene is upper limited, provided that are considered samples long enough to allow pure diffusive heat transport either for single and for collective phonon excitations. It is found that the diffusive regime is observed in samples larger than 0.1–1.0 mm. This conclusion suggests that existing experiments on suspended graphene performed on smaller samples could have been performed in a quasiballistic regime, not addressing the upper limit of intrinsic graphene thermal conductivity. The excellent agreement between AEMD and exact BTE calculations promotes AEMD as an efficient tool to investigate thermal conductivity in more realistic graphene samples, by taking into account point and extended defects as well as different chemical functionalizations.

We acknowledge G. Fugallo for useful discussions. We also acknowledge financial support by MIUR (Italy) under project PRIN 2010-2011 GRAF. Finally, C.M. acknowledges Sardinia Regional Government for financial support (P.O.R. Sardegna ESF 2007-13).

[1] A. A. Balandin, S. Ghosh, W. Bao, I. Calizo, D. Teweldebrhan, F. Miao, and C. N. Lau, Nano Lett. **8**, 902 (2008).

[2] A. A. Balandin, Nat. Mater. **10**, 569 (2011).

[3] J. H. Seol, I. Jo, A. L. Moore, L. Lindsay, Z. H. Aitken, M. T. Pettes, X. Li, Z. Yao, R. Huang, D. Broido, N. Mingo, R. S. Ruoff, and L. Shi, Science **328**, 213 (2010).

[4] D. L. Nika and A. A. Balandin, J. Phys.: Condens. Matter **24**, 233203 (2012).
[5] S. Ghosh, W. Bao, D. L. Nika, S. Subrina, E. P. Pokatilov, C. N. Lau, and A. A. Balandin, Nat. Mater. **9**, 555 (2010).
[6] R. Peierls, Ann. Phys. (Berlin) **3**, 1055 (1929).
[7] J. Callaway, Phys. Rev. **113**, 1046 (1959).
[8] P. Klemens and D. Pedraza, Carbon **32**, 735 (1994).
[9] L. Lindsay, W. Li, J. Carrete, N. Mingo, D. A. Broido, and T. L. Reinecke, Phys. Rev. B **89**, 155426 (2014).
[10] N. Bonini, J. Garg, and N. Marzari, Nano Lett. **12**, 2673 (2012).
[11] L. Paulatto, F. Mauri, and M. Lazzeri, Phys. Rev. B **87**, 214303 (2013).
[12] G. Fugallo, A. Cepellotti, L. Paulatto, M. Lazzeri, N. Marzari, and F. Mauri, Nano Lett. **14**, 6109 (2014).
[13] D. Singh, J. Y. Murthy, and T. S. Fisher, J. Appl. Phys. **110**, 044317 (2011).
[14] L. Lindsay, D. A. Broido, and N. Mingo, Phys. Rev. B **82**, 115427 (2010).
[15] W. J. Evans, L. Hu, and P. Keblinski, Appl. Phys. Lett. **96**, 203112 (2010).
[16] X. Mu, X. Wu, T. Zhang, D. B. Go, and T. Luo, Sci. Rep. **4**, 3909 (2014).
[17] Luiz Felipe C. Pereira and D. Donadio, Phys. Rev. B **87**, 125424 (2013).
[18] D. L. Nika, S. Ghosh, E. P. Pokatilov, and A. A. Balandin, Appl. Phys. Lett. **94**, 203103 (2009).
[19] D. L. Nika, E. P. Pokatilov, A. S. Askerov, and A. A. Balandin, Phys. Rev. B **79**, 155413 (2009).
[20] X. Xu, L. F. C. Pereira, Y. Wang, J. Wu, K. Zhang, X. Zhao, S. Bae, C. Tinh Bui, R. Xie, J. T. L. Thong, B. H. Hong, K. P. Loh, D. Donadio, B. Li, and B. Özyilmaz, Nat. Commun. **5**, 3689 (2014).
[21] P. K. Schelling, S. R. Phillpot, and P. Keblinski, Phys. Rev. B **65**, 144306 (2002).
[22] G. Barbarino, C. Melis, and L. Colombo, Carbon **80**, 167 (2014).
[23] B. D. Kong, S. Paul, M. B. Nardelli, and K. W. Kim, Phys. Rev. B **80**, 033406 (2009).
[24] L. Wang, B. Hu, and B. Li, Phys. Rev. E **86**, 040101 (2012).
[25] C. Melis, R. Dettori, S. Vandermeulen, and L. Colombo, Eur. Phys. J. B **87**, 96 (2014).
[26] E. Lampin, P. L. Palla, P.-A. Francioso, and F. Cleri, J. Appl. Phys. **114**, 033525 (2013).
[27] S. Plimpton, J. Comput. Phys. **117**, 1 (1995).
[28] D. W. Brenner, O. A. Shenderova, J. A. Harrison, S. J. Stuart, B. Ni, and S. B. Sinnott, J. Phys.: Condens. Matter **14**, 783 (2002).
[29] K. S. Mei, L. N. Maurer, Z. Aksamija, and I. Knezevic, J. Appl. Phys. **116**, 164307 (2014).